Journal of Materials Chemistry

Cite this: *J. Mater. Chem.*, 2011, **21**, 18681

www.rsc.org/materials

PAPER

Induced magnetism in transition metal intercalated graphitic systems

T. P. Kaloni, M. Upadhyay Kahaly* and U. Schwingenschlögl*

Received 24th July 2011, Accepted 15th September 2011
DOI: 10.1039/c1jm13527a

We investigate the structure, chemical bonding, electronic properties, and magnetic behavior of a three-dimensional graphitic network in aba and aaa stacking with intercalated transition metal atoms (Mn, Fe, Co, Ni, and Cu). Using density functional theory, we find induced spin-polarization of the C atoms both when the graphene sheets are aba stacked (forming graphite) and aaa stacked (resembling bi-layer graphene). The magnetic moment induced by Mn, Fe, and Co turns out to vary from 1.38 μ_B to 4.10 μ_B, whereas intercalation of Ni and Cu does not lead to a magnetic state. The selective induction of spin-polarization can be utilized in spintronic and nanoelectronic applications.

I. Introduction

The rich variety of the physical and chemical properties of nanoscale materials is used in a wide range of advanced technological applications. Graphene, a single layer of graphite with C atoms tightly packed in a honeycomb lattice,[1] is one of the most promising low-dimensional nanomaterials, attracting immense interest of both experimentalists and theoreticians[2,3] because of its two-dimensional (2D) structure and unique properties. In both pristine graphene and graphite no magnetic ordering is expected, by experiment and theory. However, there are various experimental methods to induce magnetism: hybridization between the C p_z and Ni d states,[4] ion implantation,[5] proton irradiation of highly oriented pyrolytic graphite,[6,7] and point defects.[8] Ferromagnetism can be induced in multi-layered graphene by randomly removing single C atoms.[9] Theoretically, spin-polarization has been confirmed for various C defects,[10–15] adsorption of molecular oxygen and hydrogen on graphene,[16] and substitutional Mn doping of graphene.[17]

Inducing spin-polarization in graphene by doping transition metal (TM) atoms[18–20] is important because it can lead to scattering[21] and modify the electronic states locally, which is required for graphene-based electronics and Kondo physics. Often, very simplistic assumptions about the effects of the TM atoms are not valid, but the properties depend strongly on the host.[22] Furthermore, precise knowledge of the TM–C interaction is important for understanding carbon nanotube growth,[23] fuel cells,[24] and the role of implanted magnetic atoms, such as Fe, for the magnetic order.[25] For these reasons it is surprising that TM intercalation in a three-dimensional (3D) graphitic network has not been studied with respect to the modifications of the interlayer interaction. In this paper, we will present first-principles results on the spin-polarization induced by Mn, Fe, Co, Ni, and Cu atoms intercalated between adjacent C layers. We study two types of stacking: aaa, which results in multilayer graphene, and aba, which results in bulk graphite. The different d valences of the TM atoms result in a range of induced magnetic moments (magnitude and spatial distribution) as needed for spintronic applications.

PSE Division, KAUST, Thuwal, 23955-6900, Kingdom of Saudi Arabia. E-mail: mousumi.upadhyaykahaly@kaust.edu.sa; udo.schwingenschlogl@kaust.edu.sa

II. Methods

Calculations based on density functional theory[26] are carried out using the generalized gradient approximation (GGA) and the plane wave Quantum-ESPRESSO code,[27] which already has been used successfully for describing graphene.[28–32] A strong corrugation of the crystal potential is present in layered materials in the direction perpendicular to the atomic planes. Consequently, the local density approximation is not valid. Even though the van-der-Waals forces are neglected in both the local density approximation and the GGA, the GGA leads to a reasonable matching of the interlayer distances with experiments and is adequate for systems with an inhomogeneous charge density.[33–35] We apply Perdew–Burke–Ernzerhof pseudopotentials[36] and include an onsite Coulomb interaction correction. In our calculations scalar relativistic effects are included, while spin–orbit coupling is not taken into account as it is negligible in the present systems. The value of the onsite interaction U is varied between 0 and 8 eV. Our results show that it is essential to use a non-zero U for the d electrons of the TM atoms. Previous findings suggest that U (which is mainly an atomic property) ranges from 1 to 5 eV for TM atoms.[37,38] For $U \geq 2$ eV our results are qualitatively similar with small variations in bond lengths and magnetic moments (< 5%). Hence, we will discuss data for $U = 4$ eV in the following, unless specifically mentioned. A large U of 8 eV leads to a reduced cohesive energy and to overestimated magnetic moments, especially in the case of Mn. All calculations are performed with a plane wave cutoff energy of 408 eV. We use

a Monkhorst–Pack[39] 16 × 16 × 4 k-mesh for the calculation of the band structure and density of states (DOS).[17,40]

We find that a 3 × 3 supercell is large enough to avoid drawbacks of the periodic boundary conditions. Our supercell contains 36 C atoms and one dopant in all cases, with a unit cell length of 7.45 Å in the *ab*-plane. The length of the *c*-axis is relaxed (~7 Å). It was suggested that the energy cost associated with the formation of two separated magnetic moments is given by the RKKY coupling between two magnetic impurities embedded in a metal, which decays slowly with the separation of the impurities in the case of a low-dimensional system. Consequently, inclusion of this effect would demand a huge unit cell with several magnetic impurities, exceeding reasonable computational resources. We fully relax the positions of all the atoms, including the dopants, in order to obtain the minimum energy configuration. We continue the optimization until an energy convergence of 10^{-7} eV per supercell and a force convergence of 0.04 eV $Å^{-1}$ is reached. To avoid trapping of TM atoms in local energy minima we have studied different starting configurations where the TM atom is located above either the bridge site (center of a C–C bond), or the hollow site (center of a C hexagon) or the top site (top of a C atom). The final lowest energy structures are tabulated in Fig. 1.

III. Structures and stability

Our data suggest that the TM atoms prefer being accommodated in different sites when intercalated in aaa and aba hosts. In aaa stacking Fe, Co, Ni, and Cu atoms tend to move towards the hollow site, while Mn atoms (smallest atomic number *Z*) prefer to remain next to a C atom and form an almost linear C–Mn–C bond. However, in aba stacking Mn, Fe, Co, and Ni atoms favor the hollow site of one C layer, which is the top site of the next C layer, see Fig. 1. Cu atoms (highest *Z*) are slightly off-centered as compared to the other atomic species.

The observed structural variations can be explained by the crystal field splittings which apply to the d orbitals of the different TM atoms. If a spatially symmetric negative charge is placed around a particular TM atom, the d orbitals remain degenerate. However, being itself negatively charged the TM atom experiences repulsion and the orbital energies are raised. As in our case the field results from electrons in the C layers on both sides of the TM atom, the charge distribution is not spherical and the degeneracy of the d orbitals is lifted. The effect is stronger for atoms with partially filled d orbitals (Fe, Co, Ni, and Cu), which thus tend to distort away from the trigonal symmetric position and form a tetrahedral-like structure with the C atoms. This is clearly visible in the left column of Fig. 1. The average C – TM – C bond angles for Mn, Fe, Co, Ni, and Cu turn out to be 180°, 143°, 151°, 144°, and 155° in aaa stacking and 143°, 139°, 141°, 141°, and 164° in aba stacking. The Mn atom, being exactly half filled, experiences only a weak effect and retains the trigonal symmetry, forming a linear C–Mn–C bond. In the aba stacking there is additional negative charge due to the C p_z orbitals. Here, the shift of neighboring C layers within the *ab*-plane offers the TM atoms a tetrahedral-like geometry. However, the unpaired electron of the Cu atom results in some off-centering.

We address the cohesive energy (E_{coh}) in Table I in order to describe the stability of the different structures. The cohesive energy per atom is defined as

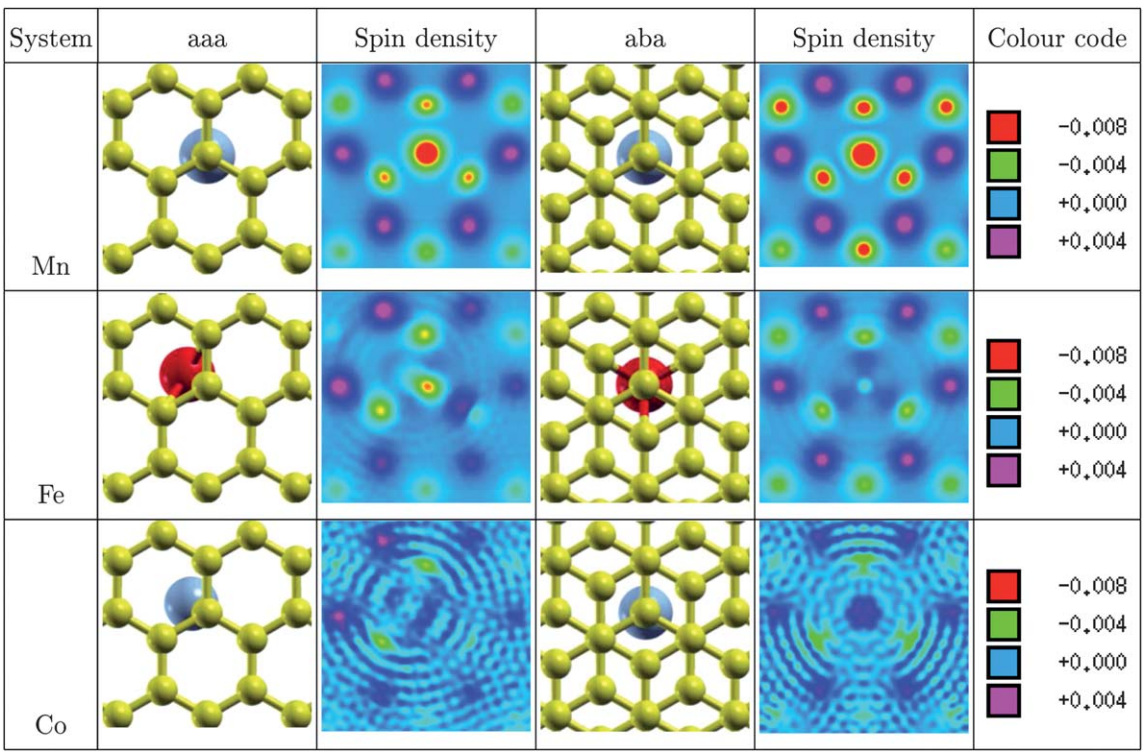

Fig. 1 Relaxed structures of the modified graphitic systems with intercalated TM atoms in aaa and aba stacking. The induced spin densities are compared to each other.

Table 1 Magnetic moment (per unit cell), average distance between dopant and nearest neighbour C atoms (l_{TM}), cohesive energy (E_{coh}), in-plane C–C bond length (l_C), bonding energy (E_b), and buckling of the graphene layers (l_B)

Stacking	Dopant	Magnetic moment/μ_B	l_{TM}/Å	E_{coh}/eV	E_b/eV	l_C/Å	l_B/Å
aaa	Mn	4.10	2.00	8.93	4.22	1.43–1.45	0.18
	Fe	3.70	2.00	8.90	3.69	1.43–1.44	0.09
	Co	1.97	2.02	8.92	4.03	1.43–1.44	0.10
	Ni	0.00	1.99	8.91	4.12	1.43–1.44	0.17
	Cu	0.00	1.98	8.82	1.13	1.43–1.45	0.01
aba	Mn	3.80	2.19	8.91	4.29	1.43–1.45	0.12
	Fe	2.06	2.17	8.89	3.42	1.43–1.45	0.01
	Co	1.83	2.26	8.92	4.15	1.43–1.45	0.08
	Ni	0.00	2.15	8.90	4.02	1.43–1.44	0.04
	Cu	0.00	2.04	8.82	0.82	1.43–1.45	0.09

$$E_{coh} = \frac{(E_{cell} - \sum E_{atom} - E_d)}{n}, \quad (1)$$

where E_{cell} is the (spin-polarized) total energy of a cell containing n atoms. E_{atom} and E_d are the total energies of isolated C and dopant atoms, respectively. They are calculated by placing a single atom in a sufficiently large cubic unit cell of ~11 Å lateral length, in order to avoid interaction with the periodic image.

The calculated magnetic moment, smallest distance between the TM atom and its nearest neighbor C atom, cohesive energy, change of the in-plane C–C bond lengths, and estimated buckling are summarized in Table I. In aaa stacking the TM–C bond length for Mn is 2.00 Å, while it varies for Fe, Co, Ni, and Cu in the ranges 2.03 to 2.26 Å, 2.01 to 2.04 Å, 1.92 to 2.18 Å, and 1.97 to 1.98 Å, respectively. In aba stacking the TM–C bond lengths for Mn vary in the range 2.00 to 2.39 Å, while for Fe, Co, Ni, and Cu we obtain 2.02 to 2.19 Å, 2.02 to 2.30 Å, 1.96 to 2.22 Å, and 1.97 to 2.19 Å, respectively. Both the bond lengths and bonding energies in Table I indicate that the bonding between the TM atoms and the C layers is covalent. A significant buckling is observed in the C layers due to the repulsion of the TM charge, amounting to 0.185 Å, 0.093 Å, 0.168 Å, 0.107 Å, and 0.098 Å (aaa stacking) and 0.118 Å, 0.015 Å, 0.079 Å, 0.044 Å, and 0.098 Å (aba stacking) for Mn, Fe, Co, Ni, and Cu, respectively. The buckling is calculated as the difference between the z-coordinates of the highest and lowest C atoms in a particular layer. The in-plane C–C bond lengths range from 1.43 Å to 1.45 Å in all structures, showing that the sp^2-hybridized nature of the in-plane bonding is retained.

IV. Electronic structure and magnetism

E_{coh} and the bonding strength decrease monotonically with increasing onsite interaction U (with a slight exception for Fe), see the top panels of Fig. 2. This has a clear but limited effect on the magnetic properties induced by the dopants, as is evident from the bottom panels of Fig. 2. We note that Mn shows a saturation of the magnetization with increasing U, consistent with ref. 17, whereas for $U = 8$ eV the magnetization trails off for Fe and Co. A growing value of U will affect more prominently the partially filled d systems Fe and Co. A choice of $U = 4$ eV is reasonable for our purpose.

In contrast to Mn doped graphene,[17] Mn intercalated graphite develops metallic states, see Fig. 3. The spin-polarized DOS for $U = 4$ eV shows that the presence of the TM enhances the DOS at the Fermi level. Both stacking schemes induce spin-polarization for Mn, Fe, and Co intercalation, amounting to 4.10 μ_B, 3.70 μ_B, and 1.97 μ_B (aaa stacking) and 3.80 μ_B, 2.06 μ_B, and 1.83 μ_B (aba stacking). Ni and Cu intercalation does not result in a magnetic state for both aaa and aba stacking. For all dopants the induced magnetic moment differs in aaa and aba stacking, due to different average C–TM bond lengths. The smaller this length, the larger is the magnetization. The spin density induced by Mn, Fe, and Co is addressed in the 3rd and 5th column of Fig. 1. The maps show localized magnetic moments on the C atoms, which reveal characteristic patterns of parallel and antiparallel orientations. When the total magnetic moment decreases along the series Mn–Fe–Co, these localized moments reduce in magnitude. However, simultaneously a weak spin density develops in the interstitial region between the atomic sites which shows a distinct circular wavy shape. This delocalized spin-polarization even dominates in the case of Co intercalation.

A Löwdin charge analysis shows that the Mn atom loses almost 0.5 electrons when it is intercalated, with d orbital occupations of ~5.5 electrons in aaa and ~5.6 electrons in aba stacking. Due to the trigonal-like crystal field around the Mn atom, the fivefold degeneracy of the d orbitals is lifted and the $d_{3z^2-r^2}$ orbital becomes almost fully occupied (in a comparatively weak crystal field). Hence, the 5.5 electrons in aaa stacking yield local magnetic moments of 3.5 μ_B to 4 μ_B, while in aba stacking

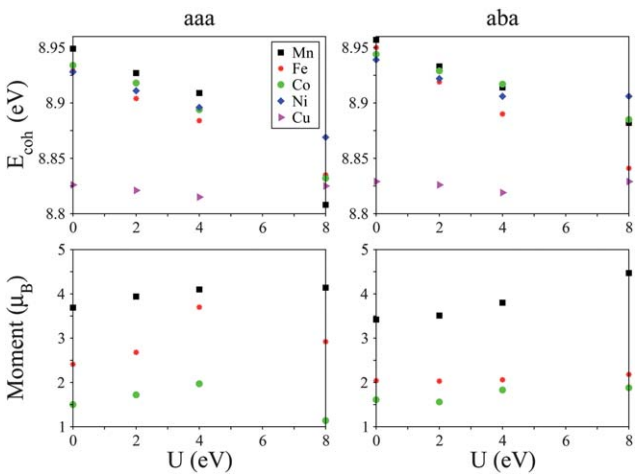

Fig. 2 Variation of the cohesive energy (E_{coh}) and total magnetic moment (per unit cell) with the onsite energy (U) in aaa and aba stacking.

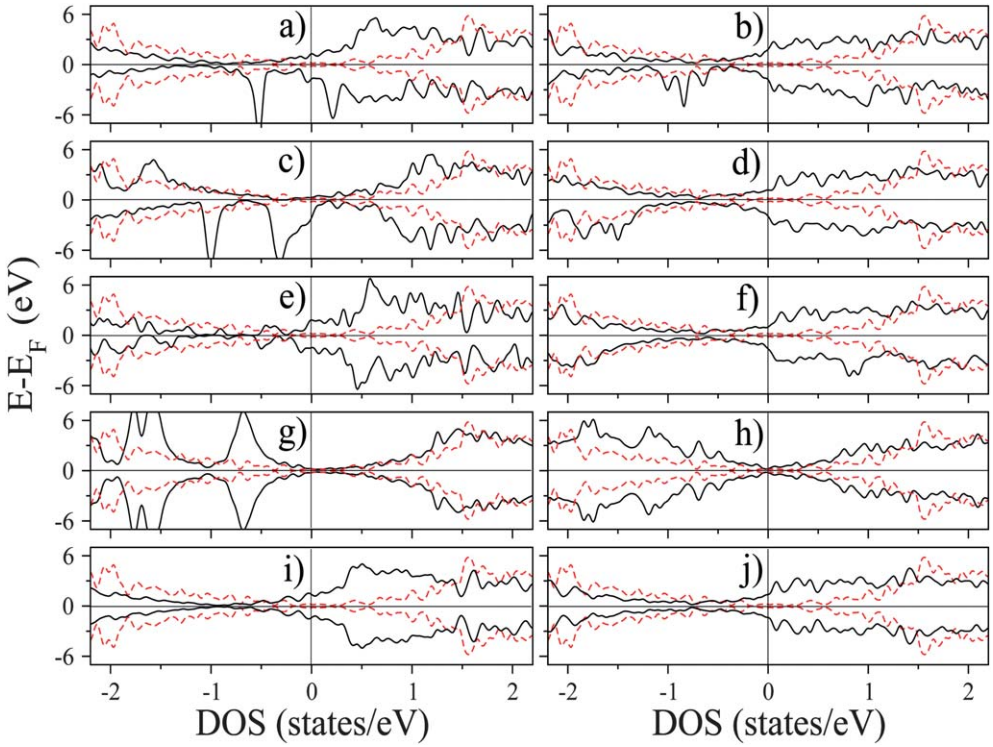

Fig. 3 Full lines: Spin majority and minority DOS obtained for the configurations (a) Mn(aaa), (b) Mn(aba), (c) Fe(aaa), (d) Fe(aba), (e) Co(aaa), (f) Co(aba), (g) Ni(aaa), (h) Ni(aba), (i) Cu(aaa), and (j) Cu(aba), where U = 4 eV. Dashed lines: Corresponding DOS for pristine graphite.

the 5.6 electrons yield a slightly smaller moment. We find that Fe loses almost 0.4 electrons in aaa and 0.3 electrons in aba stacking. The occupations of the d bands are 4.8 and 4.7, respectively. A stronger crystal field results in partial occupations of the $d_{3z^2-r^2}$, d_{xz}, and d_{yz} orbitals and total magnetic moments of 3.70 μ_B and 3.06 μ_B for aaa and aba stacking. A very strong crystal field splitting for Cu and Ni results in partial filling of all d orbitals and a prominent out-of-plane bonding of the d orbitals with the C p_z orbitals, resulting in zero magnetic moment.

Analysis of the DOS reveals that for Mn intercalation and aba stacking the states below the Fermi level reveal a strong contribution of the C p orbitals, while the states just above the Fermi energy are dominated by the Mn d orbitals. For both aaa and aba stacking, the DOS analysis suggests that the Mn atom is in a $Mn^{2-\delta}$ state, where δ is a small positive number. The partial s, p, and d occupations reflect the non-ionic character of the bonding. In the case of Fe intercalation, for both aaa and aba stacking, the states below the Fermi level are entirely due to the C p orbitals, while the lowest unoccupied states are a mixture of C p and Fe d orbitals. In case of Ni and Cu intercalation, we find that the d orbitals do not contribute to the electronic states around the Fermi level, which mainly originate from C p and TM s orbitals. This explains the non-magnetic behavior of Ni and Cu. In general a mixing of C p and TM d states points to a partially covalent character of the TM–C bond.

V. conclusion

In view of the possibility to realize a Kondo system by chemisorption of metal atoms on graphene,[41] we have addressed the behavior of the TM atoms Mn, Fe, Co, Ni, and Cu when they are intercalated in a 3D graphitic network with aaa and aba stacking. While TM adatoms on pristine graphene are reported to have bonding energies of some 0.2 eV to 1.5 eV,[42,43] we obtain bonding energies between 1.10 eV and 4.23 eV for the systems under investigation. The electronic structure of the graphitic systems is modified significantly after intercalation due to hybridization of the C p_z orbitals with the TM d orbitals. It turns out that Mn, Fe, and Co induce spin-polarization in both stacking configurations, whereas Ni and Cu result in metallic systems with zero magnetic moment. However, graphene is characterized by a high mobility of incorporated TM atoms, the strong preferential bonding of intercalated TM atoms in our case paves the way to graphitic Kondo systems.

Acknowledgements

We thank KAUST research computing for providing the computational resources used for this study.

References

1 K. S. Novoselov, A. K. Geim, S. V. Morozov, D. Jiang, Y. Zhang, S. V. Dubonos, I. V. Grigorieva and A. A. Firsov, *Science*, 2004, **306**, 666.
2 Y. Zhang, Y.-W. Tan, H. L. Stormer and P. Kim, *Nature*, 2005, **438**, 201.
3 Y.-W. Son, M. L. Cohen and S. G. Louie, *Nature*, 2006, **444**, 347.
4 M. Weser, Y. Rehder, K. Horn, M. Sicot, M. Fonin, A. B. Preobrajenski, E. N. Voloshina, E. Goering and Y. S. Dedkov, *Appl. Phys. Lett.*, 2010, **96**, 012504.

5 *Carbon-Based Magnetism: An Overview of Metal Free Carbon-Based Compounds and Materials*, edited by T. Makarova and F. Palacio (Elsevier, Amsterdam, 2005).
6 P. Esquinazi, D. Spemann, R. Höhne, A. Setzer, K.-H. Han and T. Butz, *Phys. Rev. Lett.*, 2003, **91**, 227201.
7 P. Esquinazi, Á. Setzer, R. Höhne and C. Semmelhack, *Phys. Rev. B: Condens. Matter*, 2002, **66**, 024429.
8 J. S. Črvenka, M. I. Katsnelson and C. F. J. Flipse, *Nat. Phys.*, 2009, **5**, 840.
9 M. M. Ugeda, I. Brihuega, F. Guinea and J. M. Gómez-Rodríguez, *Phys. Rev. Lett.*, 2010, **104**, 096804.
10 P. O. Lehtinen, A. S. Foster, Y. Ma, A. V. Krasheninnikov and R. M. Nieminen, *Phys. Rev. Lett.*, 2004, **93**, 187202.
11 R. Faccio, H. Pardo, P. A. Denis, R. Y. Oeiras, F. M. Araújo-Moreira, M. Veríssimo-Alves and Á. W. Mombrú, *Phys. Rev. B: Condens. Matter Mater. Phys.*, 2008, **77**, 035416.
12 Y. Zhang, S. Talapatra, S. Kar, R. Vajtai, S. K. Nayak and P. M. Ajayan, *Phys. Rev. Lett.*, 2007, **99**, 107201.
13 S. Lisenkov, A. N. Andriotis and M. Menon, *Phys. Rev. B: Condens. Matter Mater. Phys.*, 2010, **82**, 165454.
14 R. Faccio, L. Fernández-Werner, H. Pardo, C. Goyenola, O. N. Ventura and Á. W. Mombrú, *J. Phys. Chem. C*, 2010, **114**, 18961.
15 O. V. Yazyev and L. Helm, *Phys. Rev. B: Condens. Matter Mater. Phys.*, 2007, **75**, 125408.
16 J. Dai and J. Yuan, *Phys. Rev. B: Condens. Matter Mater. Phys.*, 2010, **81**, 165414.
17 M. Wu, C. Cao and J. Z. Jiang, *New J. Phys.*, 2010, **12**, 063020.
18 B. Uchoa, V. N. Kotov, N. M. R. Peres and A. H. Castro Neto, *Phys. Rev. Lett.*, 2008, **101**, 026805.
19 B. Uchoa, C.-Y. Lin and A. H. Castro Neto, *Phys. Rev. B: Condens. Matter Mater. Phys.*, 2008, **77**, 035420.
20 A. V. Krasheninnikov, P. O. Lehtinen, A. S. Foster, P. Pyykko and R. M. Nieminen, *Phys. Rev. Lett.*, 2009, **102**, 126807.
21 M. I. Katsnelson, F. Guinea and A. K. Geim, *Phys. Rev. B: Condens. Matter Mater. Phys.*, 2009, **79**, 195426.
22 H. Raebiger, S. Lany and A. Zunger, *Nature*, 2008, **453**, 763.
23 O. V. Yazyev and A. Pasquarello, *Phys. Rev. Lett.*, 2008, **100**, 156102.
24 G. Che, B. B. Lakshmi, E. R. Fisher and C. R. Martin, *Nature*, 1998, **393**, 346.
25 R. Sielemann, Y. Kobayashi, Y. Yoshida, H. P. Gunnlaugsson and G. Weyer, *Phys. Rev. Lett.*, 2008, **101**, 137206.
26 W. Kohn and L. J. Sham, *Phys. Rev.*, 1965, **140**, 1133A.
27 P. Giannozzi, *et al.*, *J. Phys.: Condens. Matter*, 2009, **21**, 395502.
28 C.-H. Park, F. Giustino, M. L. Cohen and S. G. Louie, *Nano Lett.*, 2008, **8**, 4229.
29 K. N. Kudin, B. Ozbas, H. C. Schniepp, Robert K. Prud'homme, I. A. Aksay and R. Car, *Nano Lett.*, 2008, **8**, 36.
30 A. Das, S. Pisana, B. Chakraborty, S. Piscanec, S. K. Saha, U. V. Waghmare, K. S. Novoselov, H. R. Krishnamurthy, A. K. Geim, A. C. Ferrari and A. K. Sood, *Nat. Nanotechnol.*, 2008, **3**, 210.
31 Y. C. Cheng and U. Schwingenschlögl, *Appl. Phys. Lett.*, 2010, **97**, 193304.
32 Y. C. Cheng, Z. Y. Zhu, G. S. Huang and U. Schwingenschlögl, *Phys. Rev. B: Condens. Matter Mater. Phys.*, 2011, **83**, 115449.
33 V. N. Strocov, P. Blaha, H. I. Starnberg, M. Rohlfing, R. Claessen, J.-M. Debever and J.-M. Themlin, *Phys. Rev. B: Condens. Matter*, 2000, **61**, 4994.
34 E. Konstantinova, S. O. Dantas and P. M. V. B. Barone, *Phys. Rev. B: Condens. Matter Mater. Phys.*, 2006, **74**, 035417.
35 Y. Zhang, S. Talapatra, S. Kar, R. Vajtai, S. K. Nayak and P. M. Ajayan, *Phys. Rev. Lett.*, 2007, **99**, 107201.
36 J. P. Perdew, K. Burke and M. Ernzerhof, *Phys. Rev. Lett.*, 1996, **77**, 3865.
37 P. Wei and Z. Q. Qi, *Phys. Rev. B: Condens. Matter*, 1994, **49**, 10864.
38 A. E. Bocquet, T. Mizokawa, T. Saitoh, H. Namatame and A. Fujimori, *Phys. Rev. B: Condens. Matter*, 1992, **46**, 3771.
39 H. J. Monkhorst and J. D. Pack, *Phys. Rev. B: Solid State*, 1976, **13**, 5188.
40 M. A. Khan, M. A. Mukaddam and U. Schwingenschlögl, *Chem. Phys. Lett.*, 2010, **498**, 157.
41 K. Sengupta and G. Baskaran, *Phys. Rev. B: Condens. Matter Mater. Phys.*, 2008, **77**, 045417.
42 H. Sevincli, M. Topsakal, E. Durgun and S. Ciraci, *Phys. Rev. B: Condens. Matter Mater. Phys.*, 2008, **77**, 195434.
43 K. T. Chan, J. B. Neaton and M. L. Cohen, *Phys. Rev. B: Condens. Matter Mater. Phys.*, 2008, **77**, 235430.